Table 1
Clinical data of patients with IPAH.

Patient	Time	Sex	Age	PAP (s/d/m) (mmHg)	mRAP (mmHg)	CI (L/min/m^2)	PVR (dyn/s/cm^5)	BNP (pg/dL)
1	Prior to drug therapy	F	7	150/72/98	4	3.8	1918	136
	Prior to transplantation		13	99/59/72	15	2.3	2779	334
2	Prior to drug therapy	F	28	88/40/59	10	1.9	1416	408
	Prior to transplantation		31	73/30/48	1	2.1	1199	325
3	Prior to drug therapy	F	10	118/67/84	14	2	NA	NA
	Prior to transplantation		13	111/49/67	10	1.7	2438	203
4	Prior to drug therapy	F	NA	NA	NA	NA	NA	NA
	Prior to transplantation		28	113/36/66	7	1.8	3340	50
5	Prior to drug therapy	M	16	163/71/106	2	1.7	2267	14
	Prior to transplantation		20	70/40/50	2	3.3	808	18
6	Prior to drug therapy	F	39	74/23/42	3	2.6	NA	NA
	Prior to transplantation		43	107/47/72	15	2.4	3056	622
7	Prior to drug therapy	F	13	96/50/68	4	2.3	1495	411
	Prior to transplantation		16	83/51/65	8	2.5	784	216
8	Prior to drug therapy	M	NA	NA	NA	NA	NA	NA
	Prior to transplantation		11	130/51/80	9	1.9	2629	420
Mean ± SE	Prior to drug therapy		19 ± 5	mPAP: 76 ± 10	6 ± 2	2.4 ± 0.3	1774 ± 198	242 ± 100
	Prior to transplantation		22 ± 4	mPAP: 65 ± 4	8 ± 2	2.3 ± 0.2	2129 ± 366	273 ± 70

M: male, F: female, PAP: pulmonary artery pressure, s/d/m: systolic/diastolic/mean, mRAP: mean right atrial pressure, CI: cardiac index, PVR: pulmonary vascular resistance, BNP: plasma concentration of brain natriuretic peptide, NA: not available.

is characteristic of a particular cancer cell, rather than non-specifically inhibiting the proliferation of and killing all rapidly dividing cells. Schermuly et al. reported that imatinib reverses pulmonary vascular remodeling and cor pulmonale in rats with monocrotaline-induced PH and in mice with chronic hypoxia-induced PH [8]. Perros et al. reported that PDGF-BB-induced proliferation and migration of PASMCs from patients with IPAH were inhibited by imatinib [10].

Not only inhibition of proliferation but also induction of apoptosis of PASMCs is needed to actively reduce stenosis due to vascular remodeling at small pulmonary arteries of patients with IPAH. These two effects may lead to reverse remodeling of the pulmonary vasculature. Expression of PDGF-B is up-regulated in the medial layer of small pulmonary arteries of rats with monocrotaline-induced PH and imatinib induces apoptosis in the small pulmonary arteries [8]. However, imatinib does not induce apoptosis in cultured IPAH-PASMCs without PDGF treatment [10]. Thus, imatinib may not be able to induce apoptosis in quiescent cells. We hypothesized that imatinib in the presence of PDGF-BB induces apoptosis of PASMCs from patients with IPAH, but that imatinib cannot induce apoptosis in PASMCs without PDGF stimulation. We therefore investigated whether imatinib in the presence and absence of PDGF-BB induces apoptosis of PASMCs from patients with IPAH.

Akt is a member of the serine/threonine-specific kinase family known for facilitating cell survival via the inhibition of apoptotic pathways [12]. Therefore, induction of apoptosis of IPAH-PASMCs may be related to Akt inactivation. We also investigated whether imatinib inhibits Akt activation.

2. Materials and methods

2.1. Isolation, culture and identification of PASMCs

Peripheral segments of the pulmonary artery were obtained at lung transplantation [13] from 8 patients with IPAH as previously described [5,6,14,15] (2 males and 6 females; mean age, 22 ± 4 years; age range 11–43 years) (Table 1). For normal control experiments, samples of pulmonary arteries were also obtained at lung lobectomy from a patient with bronchogenic carcinoma (male, 58 years old) who showed no evidence of PAH and received no systemic chemotherapy or radiation therapy before lung lobectomy as previously described [5,6,14,15]. Samples of the pulmonary arteries were obtained from the most distal area from the carcinoma in the resected lobe. All of the studies were approved by the Ethics Committee of Okayama University Graduate School of Medicine, Density, and Pharmaceutical Sciences, and written informed consent was obtained from all patients before the procedure. The investigation also conforms to the principles outlined in the Declaration of Helsinki.

PASMCs were isolated as described previously [5,6,14–16]. Peripheral segments of pulmonary arteries smaller than 1 mm in outer diameter were disaggregated with collagenase and cut into 2-mm-long sections, and then the adventitia and endothelial cell layers were removed. Vessels were plated on a 6-well plate with Dulbecco's modified Eagle's medium (DMEM; Gibco, Grand Island, NY, USA) supplemented with 10% fetal bovine serum (FBS; Sigma) and 0.1 mg/mL kanamycin (Sigma) and incubated in a humidified 5% CO2 atmosphere at 37 °C. The culture medium was changed every 3 days. After reaching confluence, the cells were subcultured by treatment with trypsin

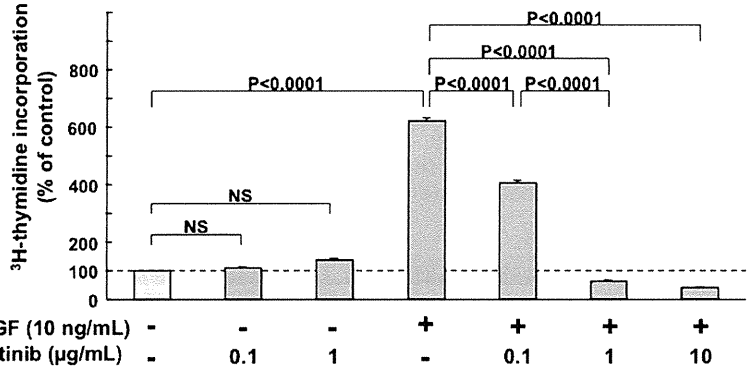

Fig. 1. Inhibitory effect of imatinib on proliferation of PASMCs from IPAH patients. Anti-proliferative effects of imatinib (0.1 to 10 μg/mL) on IPAH-PASMCs stimulated with PDGF-BB (10 ng/mL). ^{3}H-thymidine incorporation was measured. Counts per minute (cpm) were expressed as a percentage of cpm of IPAH-PASMCs treated with a diluent (control). Data are mean ± SE.

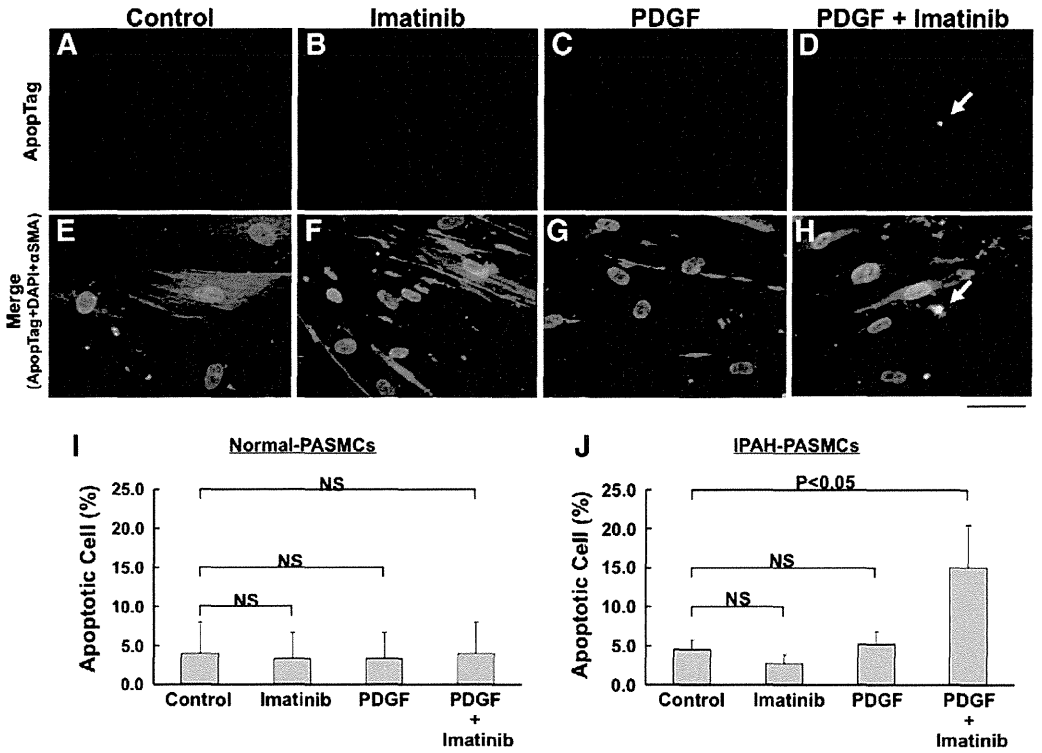

Fig. 2. Effect of imatinib on apoptosis of PASMCs in TUNEL assay by ApopTag fluorescein. A to D, ApopTag fluorescein (green). E to H, Combined images (merge) of ApopTag fluorescein, DAPI (blue) and αSMA (red). A and E, IPAH-PASMCs without treatment. B and F, IPAH-PASMCs treated with imatinib (1 μg/mL). C and G, IPAH-PASMCs treated with PDGF-BB (10 ng/mL). D and H, IPAH-PASMCs treated with imatinib and PDGF-BB. Arrow shows a TUNEL-positive cell (green). Bar = 500 μm. I, Effect of imatinib on apoptosis of normal PASMCs in TUNEL assay. J, Effect of imatinib on apoptosis of IPAH-PASMCs in TUNEL assay. Imatinib (1 μg/mL) in the presence of PDGF-BB (10 ng/mL) significantly increased TUNEL-positive (apoptotic) cells in IPAH-PASMCs compared with the control condition ($P<0.05$). Data are mean ± SE.

(0.05%)/ethylenediaminetetraacetic acid (EDTA) (0.02%). Cell identification was confirmed by the examination of cytoskeletal components (α-smooth muscle actin, myosin, and smoothelin) using an immunocytochemical technique as described previously [5,15]. Cells between passages 3 to 5 were used for all experiments.

2.2. Effects of imatinib on cell proliferation

To assess the antiproliferative effect of imatinib on PASMCs, we measured ^{3}H-thymidine incorporation using methods described previously [5,16]. PASMCs were reseeded in 24-well plates at a density of 5×10^4cells/well on day 0. After 16 h of incubation (on day 1), the culture media were replaced with low-serum culture media (DMEM, 0.1% FBS, and 0.1 mg/mL kanamycin), and the cultured cells were made quiescent for 48 h. On day 3, PDGF-BB (10 ng/mL) (Sigma), imatinib (0.1 to 10 μg/mL) (Novartis) or an Akt inhibitor, Akt-I-1/2 (1 μmol/L) (Calbiochem), was added to the media. After 21 h (on day 4), the cells were labeled with ^{3}H-thymidine at 1 μCi/mL for 3 h. After completion of labeling, the cells were washed with ice-cold PBS, fixed with 5% trichloroacetic acid and 95% ethanol, and lysed with 200 μL/well of 0.33 mol/L NaOH. Aliquots of the cell lysates were neutralized with 1 mol/L HCl, and the radioactivity was measured in a liquid scintillation analyzer (TRI-CARB 2200CA; Packard, Downers Grove, IL, USA).

2.3. Western blot analysis

PASMCs from patients with IPAH were prepared in the same manner as that described for analysis of DNA synthesis. They were treated in the presence or absence of PDGF-BB (10 or 100 ng/mL), imatinib (1 or 10 μg/mL) and a mitogen-activated protein kinase/extracellular signal-regulated kinase (MEK) inhibitor, U0126 (3 μmol/L) (Promega). Western blot analysis was performed as described previously [5,7]. Briefly, total cell lysates of cultured PASMCs were extracted in commonly used radioimmunoprecipitation (RIPA) buffer with 10 mg/mL phenylmethylsulfonyl fluoride (Sigma) and then concentrated by centrifugation at 12,000 rpm for 20 min. Protein samples (10 μg) were loaded on 10% sodium dodecyl sulfate-polyacrylamide gel and blotted onto nitrocellulose membranes. Blots were incubated with rabbit anti-p27 antibody (Santa Cruz Biotechnology), anti-GAPDH antibody (Chemicon), anti-phospho-Akt antibody and anti-total-Akt antibody (Cell Signaling Technology Inc., Beverly, MA). The relative integrated density of each protein band was digitized by NIH image J 1.34 s.

2.4. Evaluation of apoptosis

TUNEL assays were performed using an ApopTag fluorescein in situ apoptosis detection kit (Chemicon International Inc.) according to the manufacturer's instructions as described previously [17]. Nuclear morphology was examined by labeling with DAPI solution (0.6 μg/mL, Dojindo Laboratories). Immunofluorescence staining was performed to confirm α-smooth muscle actin (αSMA) expression using αSMA antibody (1:100 dilution, Sigma). Caspase assay was performed using a CaspaTag Caspase-3/7 in situ apoptosis detection kit (Chemicon International Inc.) according to the manufacturer's instructions. Nuclear morphology was examined by Hoechst staining. The samples were analyzed by fluorescence microscopy (Olympus IX71, Olympus Optical Co. Ltd, Tokyo, Japan). For each cover slip, 5–10 fields (with 10–30 cells in each field) were randomly selected to determine the percentage of apoptotic cells in total cells based on the morphological characteristics of apoptosis. PASMCs were reseeded on collagen-coated glass cover slips in 12-well plates at a density of 5×10^4 cells/well on day 0. After 16 h of incubation (on day 1), the culture media were replaced with low-serum culture media (DMEM, 0.1% FBS, and 0.1 mg/mL kanamycin), and the cultured cells were made quiescent for 48 h. On day 3, PDGF-BB (10 ng/mL), imatinib (1 μg/mL) or Akt-I-1/2 (1 μmol/L) was added to the media. After 24 h (on day 4), the cells were stained by using an ApopTag fluorescein in situ apoptosis detection kit or CaspaTag in situ apoptosis detection kit.

Transmission electron microscopy was performed with an electron microscope (H-7100: Hitachi; Tokyo, Japan).

To observe cellular apoptosis with a time-lapse system (Olympus Optical Co.), PASMCs were cultured on a 35-mm culture dish that has a micro-photolithographed squared pattern (Kuraray Co., Ltd., Tsukuba, Japan) [7] so that the apoptotic cells will not disappear from view.

2.5. Statistical analysis

All results are expressed as mean ± SE. Statistical significance for comparison between the two measurements was determined using Student's *t* test. For comparison between the different treatment groups, statistical analysis was performed using one-

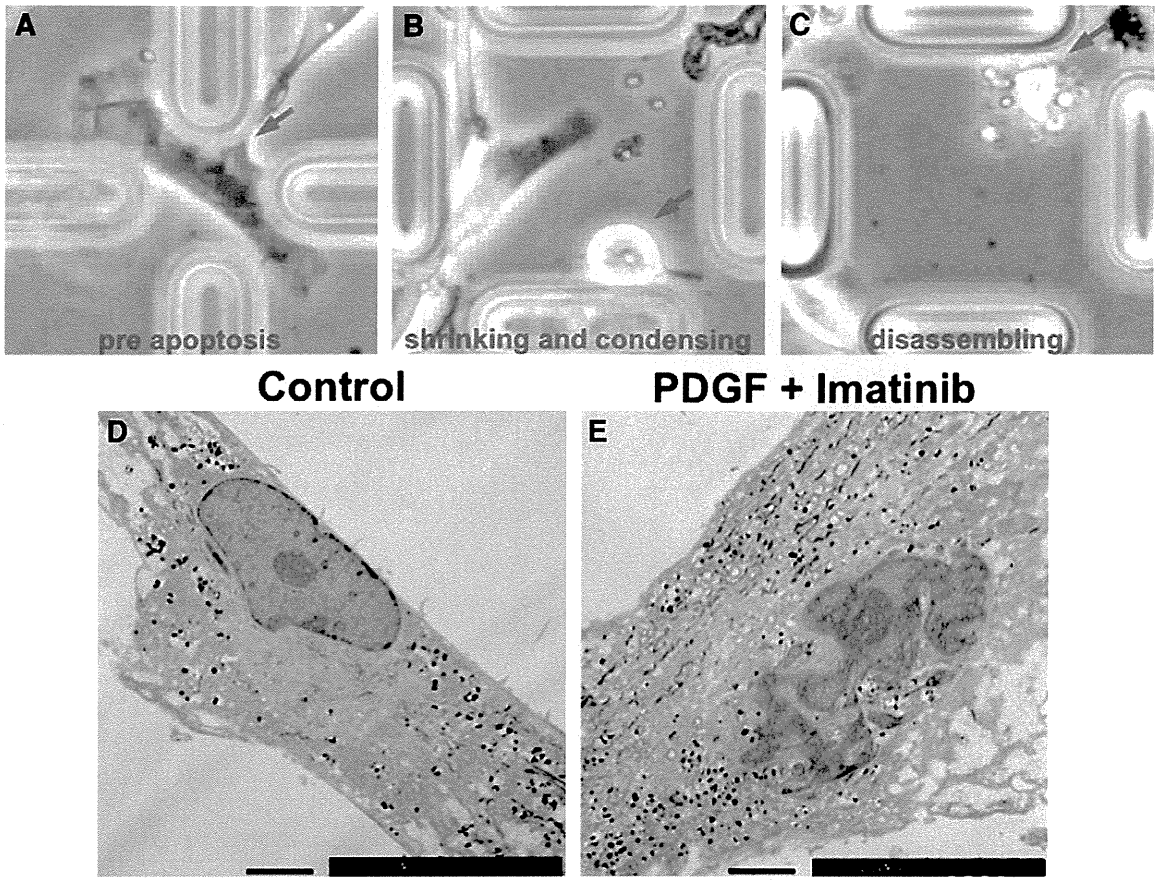

Fig. 3. Effect of imatinib on apoptosis of PASMCs in time-lapse microscopy and transmission electron microscopy. A to C, Representative images of time-lapse microscopy. IPAH-PASMCs were treated with imatinib (1 μg/mL) and PDGF-BB (10 ng/mL). Bar = 20 μm. D and E, Representative images of transmission electron microscopy. D, IPAH-PASMCs without treatment (control). E, IPAH-PASMCs treated with imatinib (1 μg/mL) and PDGF-BB (10 ng/mL). Bar = 5 μm.

way ANOVA with Fisher's PLSD test. Values of $P<0.05$ were considered to be statistically significant.

3. Results

3.1. Inhibitory effect of imatinib on proliferation of PASMCs from IPAH patients

Treatment with imatinib inhibited PDGF-BB-induced proliferation of PASMCs from IPAH patients as assessed by ^{3}H-thymidine incorporation (n = 5–12 experiments in each cell) (Fig. 1). This result is consistent with recent findings of other investigators [10].

3.2. Effect of imatinib on apoptosis of PASMCs from IPAH patients

We performed a TUNEL assay using an ApopTag fluorescein to assess the effect of imatinib on apoptosis of PASMCs from IPAH patients. Fig. 2 shows representative cases of the TUNEL assay. TUNEL-positive cell (green) was observed after 24-hour treatment with imatinib (1 μg/mL) in the presence of PDGF-BB (10 ng/mL) (Fig. 2D and H). However, imatinib (1 μg/mL) (Fig. 2B and F) or PDGF-BB (10 ng/mL) (Fig. 2C and G) alone did not induce apoptosis in IPAH-PASMCs. Imatinib (1 μg/mL) in the presence of PDGF-BB (10 ng/mL) significantly increased TUNEL-positive cells in IPAH-PASMCs compared with the control condition in IPAH-PASMCs ($P<0.05$: 15.1 ± 5.4% versus 4.5 ± 1.3%, n = 4 or 5 experiments in each cell line) (Fig. 2J). There was no significant difference in the percentage of TUNEL-positive cells between the imatinib alone or PDGF alone condition and the control condition (Fig. 2J). There was also no significant difference between the imatinib alone, PDGF alone or both imatinib and PDGF condition and the control condition in normal PASMCs (P = NS, n = 5 experiments) (Fig. 2I).

Fig. 3A, B and C shows the apoptosis induced by the combination of imatinib (1 μg/mL) and PDGF-BB (10 ng/mL) in IPAH-PASMCs as assessed by time-lapse microscopy. A PASMC shows shrinking and condensing and finally disassembling. Fig. 3E shows a transmission electron microscopic image of an apoptotic cell in IPAH-PASMCs. Condensation of chromatin along the nuclear membrane and fragmentation of the nucleus were observed in cultured IPAH-PASMCs treated with imatinib (1 μg/mL) and PDGF-BB (10 ng/mL).

Fig. 4 shows representative cases of the caspase assay in IPAH-PASMCs. Caspase-3 and −7-active cell was observed after 24-hour treatment with imatinib (1 μg/mL) in the presence of PDGF-BB (10 ng/mL) (Fig. 4D and H). Imatinib (1 μg/mL) in the presence of PDGF-BB (10 ng/mL) significantly increased caspase-3 and −7-active cells in IPAH-PASMCs compared with the control condition ($P<0.01$: 12.4 ± 3.0% versus 2.2 ± 1.2%, n = 5 experiments in each cell line) (Fig. 4J). There was no significant difference in the percentage of caspase-3 and −7-positive cells between the imatinib alone or PDGF alone condition and the control condition in IPAH-PASMCs (Fig. 4J). There was also no significant difference between the imatinib alone, PDGF alone or both imatinib and PDGF condition and the control condition in normal PASMCs (P = NS, n = 5 experiments) (Fig. 3I).

These results show that imatinib did not induce apoptosis in normal PASMCs and quiescent IPAH-PASMCs but that imatinib had a proapoptotic effect on IPAH-PASMCs stimulated with PDGF.

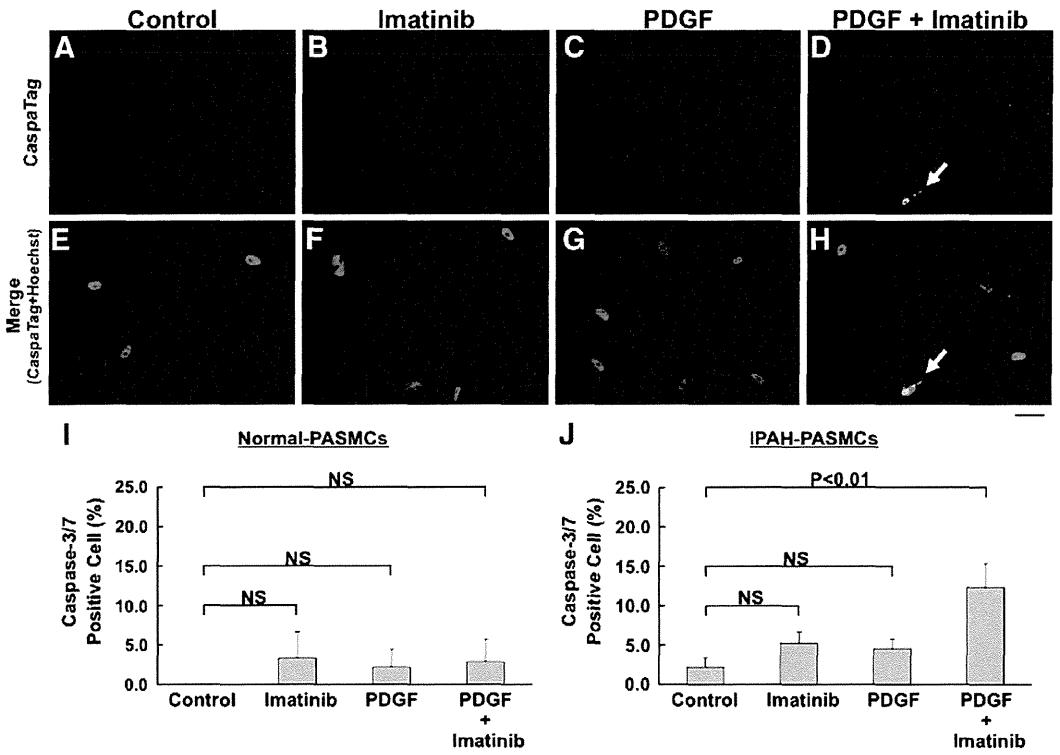

Fig. 4. Effect of imatinib on apoptosis of PASMCs in Caspase assay using a CaspaTag Caspase-3/7 in situ apoptosis detection kit. A to D, CaspaTag staining (green). E to H, Combined images (merge) of CaspaTag staining and Hoechst nuclear staining (blue). A and E, IPAH-PASMCs without treatment. B and F, IPAH-PASMCs treated with imatinib (1 μg/mL). C and G, IPAH-PASMCs treated with PDGF-BB (10 ng/mL). D and H, IPAH-PASMCs treated with imatinib and PDGF-BB. Arrow shows a caspase-3/7-positive cell (green). Bar = 500 μm. I, Effect of imatinib on apoptosis of normal PASMCs in Caspase assay. J, Effect of imatinib on apoptosis of IPAH-PASMCs in Caspase assay. Imatinib (1 μg/mL) in the presence of PDGF-BB (10 ng/mL) significantly increased caspase-positive (apoptotic) cells in IPAH-PASMCs compared with the control condition ($P<0.01$). Data are mean ± SE.

3.3. Effect of imatinib on PDGF-BB-induced phosphorylation of Akt

Western blot analysis revealed that PDGF-BB induced phosphorylation of Akt at 15 min (Fig. 5A, lanes 2 and B). Akt phosphorylation was significantly inhibited by imatinib (1 ng/mL) compared with the treatment with PDGF-BB ($P<0.05$, $n=4$ experiments) (Fig. 5A, lanes 3 and B).

Akt-I-1/2 (1 μmol/L), an Akt inhibitor, could mimic the effects of imatinib on PASMCs. Akt-I-1/2 significantly inhibited PDGF-induced proliferation of IPAH-PASMCs as assessed by ^{3}H-thymidine incorporation ($P<0.001$, $n=10$ experiments) (Fig. 5C). Akt-I-1/2 in the presence of PDGF-BB significantly increased TUNEL-positive cells ($P<0.05$, $n=5$ experiments) (Fig. 5D) and caspase-3,7-positive cells in IPAH-PASMCs ($P<0.05$, $n=5$ experiments) (Fig. 5E) compared with the control condition. These results show that the inhibition of Akt is strongly related to the anti-proliferative and pro-apoptotic effects of imatinib on PDGF-stimulated IPAH-PASMCs.

4. Discussion

Two major new findings were obtained in the present study. First, imatinib did not induce apoptosis in quiescent IPAH-PASMCs and normal PASMCs, but it had a pro-apoptotic effect on IPAH-PASMCs stimulated with PDGF. Second, inhibition of Akt is related to the anti-proliferative and pro-apoptotic effects of imatinib on PDGF-stimulated IPAH-PASMCs.

Imatinib alone did not induce apoptosis in IPAH-PASMCs. This result is consistent with recent findings of other investigators [10]. However, the combination of imatinib and PDGF induced apoptosis. Therefore, imatinib did not induce apoptosis in quiescent IPAH-PASMCs, but it had a pro-apoptotic effect on IPAH-PASMCs stimulated with PDGF. It has been reported that PDGF-A and PDGF-B mRNA levels were increased in small pulmonary arteries from patients with IPAH [10] and that serum PDGF-BB levels across the lung circulation were higher in IPAH patients [18]. Therefore, imatinib is expected to induce apoptosis in clinical settings. Further studies are needed to clarify this point.

Many signaling pathways, including ERK, p38 MAPK and Akt, are involved in proliferation and survival of PASMCs [14,19]. Akt is a member of the serine/threonine-specific kinase family known for facilitating cell survival via the inhibition of apoptotic pathways. It has been shown that PDGF stimulation transiently phosphorylates Akt and the mammalian target of rapamycin (mTOR) in PASMCs from patients with chronic thromboembolic pulmonary hypertension [19]. In our study, PDGF-BB induced phosphorylation of Akt and it was inhibited by imatinib in IPAH-PASMCs. Akt-I-1/2, an Akt inhibitor, could mimic the effects of imatinib on PASMCs. Akt is related to the anti-proliferative and pro-apoptotic effects of imatinib on PDGF-stimulated IPAH-PASMCs.

Imatinib is a drug used for treating chronic myelogenous leukemia and gastrointestinal stromal tumors. However, resistance to imatinib can occur [20–22]. Not only primary resistance within the first two months but also secondary resistance develops after a median of about 2 years of treatment with the drug. Hatano et al. reported that imatinib decreases the plasma concentration of PDGF-BB in patients with PAH, while the improvement in hemodynamic parameters is transient [11]. We showed that imatinib had a pro-apoptotic effect on IPAH-PASMCs stimulated with PDGF in the present study. Thus, imatinib would induce apoptosis only in the early period of treatment when plasma PDGF-BB levels are relatively high. After the PDGF levels have decreased, imatinib would not be able to induce apoptosis. Therefore, resistance to imatinib might occur in patients with pulmonary hypertension. Attention is needed in clinical use.

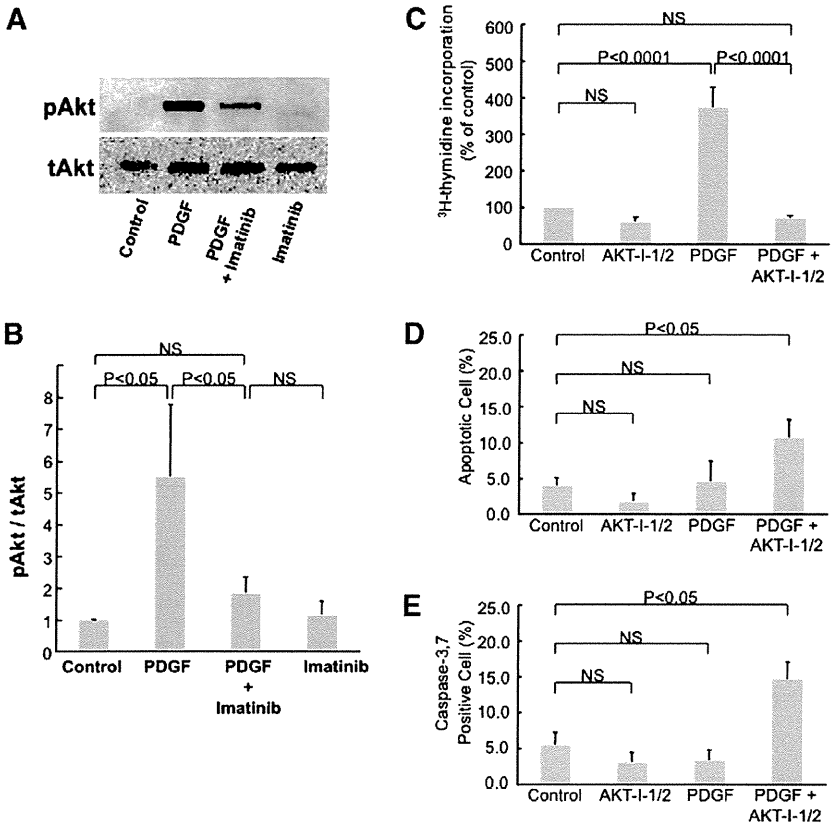

Fig. 5. Effect of imatinib on PDGF-BB-induced phosphorylation of Akt and effects of an Akt inhibitor on PDGF-BB-stimulated proliferation and apoptosis of PASMCs. A, Western blot analysis of total Akt (tAkt) and phosphorylated Akt (pAkt). PDGF-BB (10 ng/mL) induced phosphorylation of Akt at 15 min (lanes 2). Akt phosphorylation was inhibited by imatinib (1 ng/mL) (lanes 3). B, Bar graphs show semiquantitive analysis of pAkt expression level in IPAH-PASMCs. Data are mean ± SE of the intensity of the band corresponding to pAkt relative to tAkt. C, Anti-proliferative effect of Akt-I-1/2 (1 μmol/L), an Akt inhibitor, on IPAH-PASMCs stimulated with PDGF-BB (10 ng/mL). ^{3}H-thymidine incorporation was measured. Counts per minute (cpm) were expressed as a percentage of cpm of IPAH-PASMCs treated with a diluent (control). Data are mean ± SE. D, Effect of Akt-I-1/2 (1 μmol/L) on apoptosis of PASMCs in TUNEL assay by ApopTag fluorescein. E, Effect of Akt-I-1/2 (1 μmol/L) on apoptosis of PASMCs in Caspase assay using a CaspaTag Caspase-3/7 in situ apoptosis detection kit.

In conclusion, imatinib inhibited PDGF-induced proliferation of IPAH-PASMCs. Imatinib did not induce apoptosis in quiescent IPAH-PASMCs, but it had a pro-apoptotic effect on IPAH-PASMCs stimulated with PDGF. Inhibition of Akt may be important in the anti-proliferative and pro-apoptotic effects of imatinib on PDGF-stimulated IPAH-PASMCs. Modulation of PDGF signaling such as Akt is important. Inhibition of PDGF signaling by imatinib may become a useful molecular-targeted therapy for IPAH.

Conflict of interest

There are no relationships with industry.

Acknowledgments

The authors thank Kaoru Akazawa, Masayo Ohmori, and Miyuki Fujiwara for their excellent technical assistance. The authors of this manuscript have certified that they comply with the Principles of Ethical Publishing in the International Journal of Cardiology [23].

References

[1] Archer S, Rich S. Primary pulmonary hypertension: a vascular biology and translational research "Work in progress". Circulation 2000;102:2781–91.
[2] Miura A, Nakamura K, Kusano KF, et al. Three-dimensional structure of pulmonary capillary vessels in patients with pulmonary hypertension. Circulation 2010;121:2151–3.
[3] Barst RJ. PDGF signaling in pulmonary arterial hypertension. J Clin Invest 2005;115:2691–4.
[4] Barst RJ, Gibbs JS, Ghofrani HA, et al. Updated evidence-based treatment algorithm in pulmonary arterial hypertension. J Am Coll Cardiol 2009;54:S78–84.
[5] Ogawa A, Nakamura K, Matsubara H, et al. Prednisolone inhibits proliferation of cultured pulmonary artery smooth muscle cells of patients with idiopathic pulmonary arterial hypertension. Circulation 2005;112:1806–12.
[6] Fujio H, Nakamura K, Matsubara H, et al. Carvedilol inhibits proliferation of cultured pulmonary artery smooth muscle cells of patients with idiopathic pulmonary arterial hypertension. J Cardiovasc Pharmacol 2006;47:250–5.
[7] Ikeda T, Nakamura K, Akagi S, et al. Inhibitory effects of simvastatin on platelet-derived growth factor signaling in pulmonary artery smooth muscle cells from patients with idiopathic pulmonary arterial hypertension. J Cardiovasc Pharmacol 2010;55:39–48.
[8] Schermuly RT, Dony E, Ghofrani HA, et al. Reversal of experimental pulmonary hypertension by PDGF inhibition. J Clin Invest 2005;115:2811–21.
[9] Ghofrani HA, Seeger W, Grimminger F. Imatinib for the treatment of pulmonary arterial hypertension. N Engl J Med 2005;353:1412–3.
[10] Perros F, Montani D, Dorfmuller P, et al. Platelet-derived growth factor expression and function in idiopathic pulmonary arterial hypertension. Am J Respir Crit Care Med 2008;178:81–8.
[11] Hatano M, Yao A, Shiga T, Kinugawa K, Hirata Y, Nagai R. Imatinib mesylate has the potential to exert its efficacy by down-regulating the plasma concentration of platelet-derived growth factor in patients with pulmonary arterial hypertension. Int Heart J 2010;51:272–6.
[12] Wendel HG, De Stanchina E, Fridman JS, et al. Survival signalling by Akt and eIF4E in oncogenesis and cancer therapy. Nature 2004;428:332–7.
[13] Date H, Kusano KF, Matsubara H, et al. Living-donor lobar lung transplantation for pulmonary arterial hypertension after failure of epoprostenol therapy. J Am Coll Cardiol 2007;50:523–7.
[14] Takeda M, Otsuka F, Nakamura K, et al. Characterization of the bone morphogenetic protein (BMP) system in human pulmonary arterial smooth muscle cells isolated from a sporadic case of primary pulmonary hypertension: roles of BMP type IB receptor (activin receptor-like kinase-6) in the mitotic action. Endocrinology 2004;145:4344–54.
[15] Nakamura K, Shimizu J, Kataoka N, et al. Altered nano/micro-order elasticity of pulmonary artery smooth muscle cells of patients with idiopathic pulmonary arterial hypertension. Int J Cardiol 2010;140:102–7.

[16] Kouchi H, Nakamura K, Fushimi K, et al. Manumycin A, inhibitor of ras farnesyltransferase, inhibits proliferation and migration of rat vascular smooth muscle cells. Biochem Biophys Res Commun 1999;264:915–20.
[17] Nikaido A, Tada T, Nakamura K, et al. Clinical features of and effects of angiotensin system antagonists on amiodarone-induced pulmonary toxicity. Int J Cardiol 2010;140:328–35.
[18] Selimovic N, Bergh CH, Andersson B, Sakiniene E, Carlsten H, Rundqvist B. Growth factors and interleukin-6 across the lung circulation in pulmonary hypertension. Eur Respir J 2009;34:662–8.
[19] Ogawa A, Firth AL, Yao W, et al. Inhibition of mTOR attenuates store-operated Ca^{2+} entry in cells from endarterectomized tissues of patients with chronic thromboembolic pulmonary hypertension. Am J Physiol Lung Cell Mol Physiol 2009;297: L666–76.
[20] Kantarjian H, Giles F, Wunderle L, et al. Nilotinib in imatinib-resistant CML and Philadelphia chromosome-positive ALL. N Engl J Med 2006;354:2542–51.
[21] Demetri GD, von Mehren M, Blanke CD, et al. Efficacy and safety of imatinib mesylate in advanced gastrointestinal stromal tumors. N Engl J Med 2002;347: 472–80.
[22] Verweij J, Casali PG, Zalcberg J, et al. Progression-free survival in gastrointestinal stromal tumours with high-dose imatinib: randomised trial. Lancet 2004;364:1127–34.
[23] Shewan LG, Coats AJ. Ethics in the authorship and publishing of scientific articles. Int J Cardiol 2010;144:1–2.

Journal of Clinical Anesthesia (2012) 24, 487–489

ELSEVIER

Journal of Clinical Anesthesia

Case Report

Scheduled perioperative switch from oral sildenafil to intravenous epoprostenol in a patient with Eisenmenger syndrome undergoing a sigmoidectomy

Kiyoshi Moriyama MD (Assistant Professor of Anesthesiology)[a,*], Koji Uzawa MD (Staff Anesthesiologist)[a], Takehiko Iijima PhD, DMSc, DDS (Professor of Anesthesiology)[b], Mariko Kotani MD (Staff Anesthesiologist)[a], Kumi Moriyama MD (Assistant Professor of Anesthesiology)[a], Yuki Ohashi MD (Staff Anesthesiologist)[a], Toru Satoh MD, PhD (Professor, Second Department of Internal Medicine)[c], Tomoko Yorozu MD, PhD (Professor and Chairperson of Anesthesiology)[a]

[a]*Department of Anesthesiology, Kyorin University Faculty of Medicine, Tokyo 181–8611, Japan*
[b]*Department of Anesthesiology, Showa University School of Dentistry, Tokyo 142–8555, Japan*
[c]*Second Department of Internal Medicine, Kyorin University Faculty of Medicine, Tokyo 181–8611, Japan*

Received 3 October 2010; revised 14 January 2012; accepted 5 February 2012

Keywords:
Eisenmenger syndrome;
Epoprostenol;
Sigmoidectomy;
Sildenafil

Abstract The perioperative management of pulmonary hypertension in a patient with Eisenmenger syndrome, the most advanced form of associated pulmonary artery hypertension (PAH), who required a sigmoidectomy is presented. The treatment for pulmonary hypertension was switched from oral sildenafil to intravenous epoprostenol to avoid the unexpected discontinuation of vasodilation during the perioperative period. The scheduled perioperative conversion should be considered for patients with severe PAH undergoing major abdominal surgery to ensure the stabilization of pulmonary and systemic hemodynamics.

1. Introduction

Pulmonary artery hypertension (PAH) is a progressively fatal disease that is associated with significant perioperative respiratory and right-sided heart failure [1,2], leading to a high mortality rate of 7% within 30 days [3]. The perioperative management of pulmonary hypertension in a patient with Eisenmenger syndrome undergoing major abdominal surgery with a scheduled switch from oral sildenafil to intravenous (IV) epoprostenol is presented.

2. Case report

A 52 year old man was diagnosed with sigmoid colon cancer. This patient had an atrial septal defect (ASD) with

* Correspondence and reprint requests: Kiyoshi Moriyama, MD, Department of Anesthesiology, Kyorin University School of Medicine, 6-20-2 Shinkawa, Mitaka, Tokyo 181–8611, Japan. Tel.: +81 422 47 5511; fax: +81 422 43 1504.
E-mail address: mokiyo@ks.kyorin-u.ac.jp (K. Moriyama).

0952-8180/$ – see front matter
doi:10.1016/j.jclinane.2012.02.005

patch closure at the age of 7 years. At age 45 years, he developed dyspnea with exertion. At the age of 50, he was diagnosed with PAH after cardiac catheterization and was started on oral sildenafil treatment. At the age of 52 years, the patient was diagnosed with sigmoid colon cancer and an elective sigmoidectomy was proposed, as the patient exhibited New York Heart Association functional class II (NYHA class II) symptoms. Preoperative cardiac catheterization showed severe PAH with a pulmonary artery (PA) systolic pressure of 76/28 (mean 46 mmHg) mmHg. Pulmonary vascular resistance was 7.9 Wood units, which had decreased from his initial value of 8.8 Wood units after 18 months of oral sildenafil treatment. A preoperative transesophageal echocardiogram showed a defect with a diameter of 9 mm close to the tip of the closed ASD that was functioning as a bidirectional shunt. The step-up of oxygenation was noted at the inferior vena cava. The estimated ratio of measured pulmonary blood flow to systemic blood flow was 1.1 to 1.2. The degree of tricuspid regurgitation was moderate, with right ventricular (RV) enlargement and hypertrophy.

As the oral intake of sildenafil would be restricted for a minimum of three days after abdominal surgery, we planned a switch from oral sildenafil to IV epoprostenol. The patient was admitted to the hospital 9 days prior to the procedure. A central venous catheter was inserted via the right internal jugular vein, and the IV administration of epoprostenol was initiated at 1.0 ng/kg/min. The dose was increased daily by 1.0 ng/kg/min, and oral sildenafil was discontinued because the patient complained of a headache when epoprostenol was infused at 3.0 ng/kg/min. The patient's brain natriuretic peptide level was 80.3 pg/mL on admission, which decreased to 20.4 pg/mL after three days of epoprostenol infusion. The epoprostenol infusion was subsequently increased to 9 ng/kg/min.

On the day of the procedure, a 22-gauge catheter was inserted into the patient's left radial artery and a FloTrac® sensor (Edwards Life Sciences, Irvine, CA, USA) was connected to monitor his cardiac output. As his PaO_2 on room air was 70 mmHg, oxygen was administered at a rate of 5 L/min while a thoracic epidural catheter was placed at the Th_{10}-Th_{11} interspace. General anesthesia was induced with 50 μg of fentanyl, 70 mg of propofol, and 60 mg of rocuronium. To reduce hemodynamic instability during endotracheal intubation, an AirwayScope® (Pentax, Tokyo, Japan) was used instead of a Macintosh laryngoscope. To continuously monitor perioperative central venous oxygen saturation ($ScvO_2$), a PreSep® central venous oximetry catheter (Edwards Life Sciences) was inserted into his left jugular vein in addition to the central venous catheter. To avoid hypotension, phenylephrine was continuously infused at a rate of 0.1 to 0.5 mg/hr. General anesthesia was maintained with oxygen, air, and sevoflurane. To establish epidural anesthesia, 0.2% of ropivacaine was used. The epoprostenol infusion was maintained unchanged at 9 ng/kg/min in the operating room. During the procedure, systolic blood pressure ranged from 70 mmHg to 120 mmHg, whereas heart rate ranged from 55 bpm to 70 bpm, central venous pressure from 6 mmHg to 8 mmHg, $ScvO_2$ from 65% to 75%, and cardiac index from 2.2 L/min to 3.5 L/min. After 134 minutes of surgery and 207 minutes of general anesthesia, the patient was extubated and transferred to the intensive care unit.

The continuous infusion of phenylephrine was discontinued on the following day. The epoprostenol infusion was gradually decreased to 4 ng/kg/min on postoperative day (POD) 7. Oral intake was started on POD 4, and oral sildenafil was restarted on POD 7. On POD 9, epoprostenol was discontinued and the central venous catheter was withdrawn. The patient was discharged from the hospital on POD 15.

3. Discussion

Pulmonary hypertension associated with congenital systemic-to-pulmonary shunts is categorized as associated PAH (APAH) [4]. In patients with congenital systemic-to-pulmonary shunts, the persistent exposure of the pulmonary vasculature to increased blood flow and pressure may result in typical pulmonary obstructive arteriopathy, which leads to an increase in PVR. The most advanced form of APAH with congenital systemic-to-pulmonary shunts, described as Eisenmenger syndrome, is a condition with a reversed or bidirectional shunt [5]. The perioperative mortality rate for patients with Eisenmenger syndrome is understandably high, with a mortality rate of 24% for major surgical procedures [6]. Our patient had a bidirectional shunt and increased pulmonary artery pressure (PAP), suggesting that he had developed Eisenmenger syndrome.

The treatment for PAH has improved since the American College of Chest Physicians published their guidelines in 2004 [7], with the regulatory approval of newer drugs and accumulating experience with combinations of existing drugs [8]. Oral sildenafil significantly improves symptomatic status, exercise capacity, NYHA class, and hemodynamic parameters of patients with severe PAH [9]. Although our patient developed Eisenmenger syndrome, his daily activity level was well managed at a NYHA class I level with oral sildenafil treatment. Based on his daily activity level, we expected that he would be able to tolerate the surgical stress of a sigmoidectomy. The patient had an increased PAP with RV hypertrophy, which are univariate predictors of early postoperative mortality for patients with PAH [3]. In addition, major abdominal surgery is classified as an intermediate to high-risk surgery, which is an independent predictor of short-term morbidity and the length of hospital stay after noncardiac surgery [3]. The duration of anesthesia was expected to exceed three hours, which was another independent predictor of short-term morbidity [3]. The biggest concern for the perioperative management of his

PAH was the restriction of oral intake. To overcome these problems, a perioperative switch from oral sildenafil to IV epoprostenol was planned and initiated in advance of the surgical procedure.

Epoprostenol (synthetic prostacyclin) is the first drug to be approved by the Food and Drug Administration for the treatment of primary pulmonary hypertension. Epoprostenol is unique in that it improved the survival of patients with idiopathic PAH in a randomized study [10]. Long-term, persistent efficacy also has been shown in patients with idiopathic PAH as well as other APAH conditions [11]. The therapy is complicated, requiring the permanent placement of a tunneled central venous catheter and posing an ever-present risk of line infection. The abrupt discontinuation of infusion may be harmful because of the pharmacological instability of this drug arising from its short half-life. For practical use in daily life, the transition from epoprostenol infusion to oral therapy has been attempted [12]. Intravenous epoprostenol has been considered not only for chronic use but also perioperative use [13]. A scheduled switch from sildenafil to epoprostenol may be beneficial for perioperative management to avoid the unexpected discontinuation of vasodilation during the perioperative period.

Our patient complained of a severe headache during the transition period between the two drugs. Otherwise, he smoothly transitioned from oral sildenafil to IV epoprostenol within 9 days. Since his postoperative recovery was uneventful, without gastrointestinal complications, the IV epoprostenol was smoothly transitioned to oral sildenafil within 9 days. The patient's postoperative course was uneventful, without respiratory or RV failure, and additive therapy for pulmonary hypertension was not required. Although the hospitalization period may be prolonged because of titration, a scheduled perioperative conversion from oral sildenafil to IV epoprostenol should be considered for patients with severe PAH undergoing major abdominal surgery for the stabilization of pulmonary and systemic hemodynamics.

References

[1] Blaise G, Langleben D, Hubert B. Pulmonary arterial hypertension: pathophysiology and anesthetic approach. Anesthesiology 2003;99: 1415-32.

[2] Gordon C, Collard CD, Pan W. Intraoperative management of pulmonary hypertension and associated right heart failure. Curr Opin Anaesthesiol 2010;23:49-56.

[3] Ramakrishna G, Sprung J, Ravi BS, Chandrasekaran K, McGoon MD. Impact of pulmonary hypertension on the outcomes of noncardiac surgery: predictors of perioperative morbidity and mortality. J Am Coll Cardiol 2005;45:1691-9.

[4] Galiè N, Hoeper MM, Humbert M, et al. ESC Committee for Practice Guidelines (CPG). Guidelines for the diagnosis and treatment of pulmonary hypertension: The Task Force for the Diagnosis and Treatment of Pulmonary Hypertension of the European Society of Cardiology (ESC) and the European Respiratory Society (ERS), endorsed by the International Society of Heart and Lung Transplantation (ISHLT). Eur Heart J 2009;30:2493-537.

[5] Beghetti M, Galiè N. Eisenmenger syndrome: a clinical perspective in a new therapeutic era of pulmonary arterial hypertension. J Am Coll Cardiol 2009;53:733-40.

[6] Martin JT, Tautz TJ, Antognini JF. Safety of regional anesthesia in Eisenmenger's syndrome. Reg Anesth Pain Med 2002;27:509-13.

[7] McLaughlin VV, Presberg KW, Doyle RL, et al; American College of Chest Physicians. Prognosis of pulmonary arterial hypertension: ACCP evidence-based clinical practice guidelines. Chest 2004;126:78S-92S.

[8] Badesch DB, Abman SH, Simonneau G, Rubin LJ, McLaughlin VV. Medical therapy for pulmonary arterial hypertension: updated ACCP evidence-based clinical practice guidelines. Chest 2007;131:1917-28.

[9] Singh TP, Rohit M, Grover A, Malhotra S, Vijayvergiya R. A randomized, placebo-controlled, double-blind, crossover study to evaluate the efficacy of oral sildenafil therapy in severe pulmonary artery hypertension. Am Heart J 2006;151:851.e1-5.

[10] McLaughlin VV, Shillington A, Rich S. Survival in primary pulmonary hypertension: the impact of epoprostenol therapy. Circulation 2002;106:1477-82.

[11] Rosenzweig EB, Kerstein D, Barst RJ. Long-term prostacyclin for pulmonary hypertension with associated congenital heart defects. Circulation 1999;99:1858-65.

[12] Steiner MK, Preston IR, Klinger JR, et al. Conversion to bosentan from prostacyclin infusion therapy in pulmonary arterial hypertension: a pilot study. Chest 2006;130:1471-80.

[13] Braun EB, Palin CA, Hogue CW. Vasopressin during spinal anesthesia in a patient with primary pulmonary hypertension treated with intravenous epoprostenol. Anesth Analg 2004;99:36-7.

Sleep Breath (2012) 16:473–481
DOI 10.1007/s11325-011-0528-7

ORIGINAL ARTICLE

Analysis of anatomical and functional determinants of obstructive sleep apnea

Kensaku Aihara · Toru Oga · Yuka Harada · Yuichi Chihara · Tomohiro Handa · Kiminobu Tanizawa · Kizuku Watanabe · Takefumi Hitomi · Tomomasa Tsuboi · Michiaki Mishima · Kazuo Chin

Received: 19 November 2010 / Revised: 7 April 2011 / Accepted: 4 May 2011 / Published online: 15 May 2011

Abstract
Purpose Craniofacial abnormalities have an important role in the occurrence of obstructive sleep apnea (OSA) and may be particularly significant in Asian patients, although obesity and functional abnormalities such as reduced lung volume and increased airway resistance also may be important. We conducted simultaneous analyses of their interrelationships to evaluate the relative contributions of obesity, craniofacial structure, pulmonary function, and airway resistance to the severity of Japanese OSA because there are little data in this area.
Methods A cross-sectional observational study was performed on 134 consecutive Japanese male patients. A sleep study, lateral cephalometry, pulmonary function tests, and impulse oscillometry (IOS) were performed on all patients.
Results Age, body mass index (BMI), position of the hyoid bone, and proximal airway resistance on IOS (R20) were significantly related to the apnea/hypopnea index (AHI) ($p<0.05$) in multiple regression analysis. Subgroup analysis showed that, for moderate-to-severe OSA (AHI≥15 events/h), neck circumference and R20 were predominantly related to AHI, whereas for non-to-mild OSA (AHI<15 events/h), age and expiratory reserve volume were the predominant determinants. In obese subjects (BMI≥25 kg/m^2), alveolar–arterial oxygen tension difference, position of the hyoid bone, and R20 were significantly associated with AHI, whereas age alone was a significant factor in nonobese subjects (BMI<25 kg/m^2).
Conclusions Aside from age and obesity, anatomical and functional abnormalities are significantly related to the severity of Japanese OSA. Predominant determinants of AHI differed depending on the severity of OSA or the magnitude of obesity.

Keywords Obstructive sleep apnea · Obesity · Cephalometry · Pulmonary function · Impulse oscillometry

Introduction

Obstructive sleep apnea (OSA) is characterized by repetitive episodes of upper airway obstruction. The critical pathophysiological feature of OSA is sleep-related narrowing or closure of the upper airway at the level of the pharynx [1, 2]. Anatomical abnormality is an important risk factor for OSA, and most patients with OSA have craniofacial abnormalities such as a small mandible, enlarged tongue, enlarged soft palate, inferior displacement of the hyoid bone, and imbalance between soft tissue volume and bony enclosure size [3–5]. Dempsey et al. [6] analyzed the interactive effects of obesity and craniofacial structure on sleep-disordered breathing and reported that body mass index (BMI) and cephalometric dimensions equally contributed to the elevated apnea/hypopnea index (AHI). However, a recent study showed that craniofacial

Electronic supplementary material The online version of this article (doi:10.1007/s11325-011-0528-7) contains supplementary material, which is available to authorized users.

K. Aihara · Y. Harada · Y. Chihara · T. Handa · K. Tanizawa · K. Watanabe · M. Mishima
Department of Respiratory Medicine,
Graduate School of Medicine, Kyoto University,
Kyoto, Japan

T. Oga (✉) · T. Hitomi · T. Tsuboi · K. Chin
Department of Respiratory Care and Sleep Control Medicine,
Graduate School of Medicine, Kyoto University,
54 Kawahara, Shogoin, Sakyo-ku,
Kyoto 606-8507, Japan
e-mail: ogato@kuhp.kyoto-u.ac.jp

structure and obesity contributed differently to OSA between Caucasian and Asian patients [7]. In addition, Dempsey et al. pointed out some additional factors that might explain elevations in the AHI and speculated that functional abnormalities such as impaired neural control of upper airway muscles and ventilatory instability, which may cause increased airway resistance, might be candidates [6].

It has been shown that pharyngeal patency in OSA patients is lung volume dependent [8, 9], and previous reports indicated a significant correlation between a reduced lung volume and nocturnal obstructive apnea and desaturation [10, 11]. Increased upper airway resistance also was shown to play a role in the pathogenesis of OSA [12, 13] through the association with increased susceptibility of airway narrowing and collapse [2, 14]. Thus, in addition to anatomical abnormalities, functional abnormalities such as reduced lung volume and increased airway resistance have been shown to play important roles in the pathogenesis of OSA.

Obesity, the most important risk factor for OSA, is known to affect craniofacial structures [15], lung volume [16], and airway resistance [17, 18]. However, given the substantial number of nonobese OSA patients in Japan [19], we hypothesized that there would be significant relationships between OSA and anatomical and functional factors as well as obesity, reflecting a multi-factorial pathophysiological feature of OSA. Therefore, in the present study, we simultaneously analyzed the interrelationships among craniofacial structure, pulmonary function, airway resistance, obesity, and OSA to investigate the relative contributions of these factors to the severity of OSA.

Materials and methods

Study subjects

We performed a cross-sectional observational study of 134 consecutive Japanese male patients who visited the Sleep Unit of Kyoto University Hospital between January 2009 and February 2010 for evaluation of OSA. None had been previously diagnosed with or treated for OSA. Patients with pulmonary diseases such as asthma or chronic obstructive pulmonary disease and who were diagnosed as having central sleep apnea were excluded. This study was approved by the Kyoto University Graduate School and Faculty of Medicine Ethics Committee, and informed consent was obtained from all patients. A sleep study, lateral cephalometry, pulmonary function tests, and impulse oscillometry (IOS) were performed on all patients. To establish smoking history, the Brinkman index was calculated by the following formula:

$$\text{Brinkman index} = \text{number of cigarettes smoked per day} \times \text{number of smoking years.}$$

Arterial blood gas analysis, including arterial partial pressure of oxygen (PaO_2) and arterial partial pressure of carbon dioxide ($PaCO_2$), was performed with patients' breathing room air at rest in the supine position at 19:00. Alveolar–arterial oxygen tension difference ($A\text{-}aDO_2$) was calculated according to the standard formula, using the respiratory exchange ratio of 0.8.

Polysomnography

Diagnosis of OSA was confirmed by polysomnography (SomnoStar pro, Cardinal Health, Dublin, OH, USA), which was started at 22:00 and ended at 6:00 the following morning. Surface electrodes were attached using standard techniques to obtain an electrooculogram, electromyogram of the chin, and 12-lead electroencephalograph. Sleep stages were defined according to the criteria of Rechtschaffen and Kales [20]. Ventilation was monitored by inductive plethysmography (Respitrace QDC, Viasys Healthcare, Palm Springs, CA, USA). Airflow was monitored by a nasal air pressure transducer (PTAFlite, Pro-Tech Services Inc., Mukilteo, WA, USA) and supplemented by an oronasal thermal sensor (Sleepmate Technologies, Midlothian, VA, USA). Arterial oxygen saturation (SpO_2) was monitored continuously with a pulse oximeter (Adult Flex System, Nonin Medical, Plymouth, MN, USA).

Apnea was defined as the complete cessation of airflow and hypopnea as a clear decrease in airflow of 30% or more lasting for 10 s or more, accompanied by a decrease in SpO_2 of at least 4% [21]. All AHI values were expressed as the number of episodes of apnea and hypopnea per hour over the total sleep time. The lowest SpO_2 during sleep and the percentage of time of SpO_2 90% during sleep also were calculated in each patient. OSA severity was defined by the AHI as follows: non-OSA ($AHI<5$), mild OSA ($5\leq AHI<15$), moderate OSA ($15\leq AHI<30$), and severe OSA ($AHI\geq 30$).

Cephalometry

A lateral cephalogram was obtained for each subject. The cephalograms were taken on image plates (ST-VI, Fuji Medical Systems, Tokyo, Japan) with the subject in the sitting position at a film focus distance of 2 m, with a left to right view. Exposures were made at 75 kV and 320 mA at the end-expiratory phase during quiet breathing through the

nose, and a cephalostat was used to keep the subject's head in a position such that the Frankfort horizontal line was parallel to the floor during exposure. Images of the cephalograms were digitized and input into a computer, previewed and processed for sharp visibility of both the soft tissues and bony structures, and printed out through a computed radiography system (FCR Profect CS, Fuji Medical Systems). A total of 22 variables related to both craniofacial skeletal and soft tissue morphology were measured as angular (degrees), linear (millimeters), or area (square centimeters) by a single observer in a single-blind manner. Images were analyzed using Image J software (US NIH, Bethesda, MD, USA). Every measurement was made by the same observer, who had no knowledge of the clinical status of the patient.

The cephalometric landmarks and reference lines are defined in Table 1 and illustrated anatomically in Fig. 1. The following angles and dimensions were measured: SNA, antero-posterior position of the maxilla in relation to the anterior cranial base (angle between S–N and N–A); SNB, antero-posterior position of the mandible in relation to the anterior cranial base (angle between S–N and N–B); ANB, relative position of the mandible to the maxilla (angle between N–A and N–B); facial axis, vertical position of the mandible in relation to the skull (angle between Pt–Gn and N–Ba); G–VL, antero-posterior position of the chin in relation to the vertebra (linear distance along the perpendicular plane from G to VL); N–Ba, the length of the cranial base (distance between N and Ba); S–N, the length of the anterior cranial base (distance between S and N); ANS–PNS, the length of the hard palate (distance between ANS and PNS); PNS–Ba, bony nasopharynx (distance between PNS and Ba); PNS–P, the length of the soft palate (distance between PNS and P); PNS–V, the length of the pharyngeal airway (distance between PNS and V); MPT, greatest thickness of the soft palate; TGL, the length of the tongue (distance between V and TT); TGH, height of the tongue (linear distance along the perpendicular bisector of the V–TT line to the tongue dorsum); Me–Go, the length of the mandible (distance between Me and Go); MP–H, vertical position of the hyoid bone (linear distance along the perpendicular plane from H to MP); H–VL, antero-posterior position of the hyoid bone (linear distance along the perpendicular plane from H to VL); AW1, upper oropharyngeal airway caliber (narrowest part of the airway between PNS and P); AW2, lower oropharyngeal airway caliber (narrowest part of the airway between P and Go); airway area, dimensions of the oropharynx (area outlined by the inferior border of the nasopharynx, the posterior surface of the soft palate and tongue, the line parallel to the palatal plate through the point V, and the posterior pharyngeal wall); tongue area, dimensions of the tongue (area outlined by the dorsal aspect of the tongue surface and lines that join TT, G, H, and V); and the lower face cage,

Table 1 Definitions of cephalometric landmarks and reference lines

S	Sella, midpoint of the fossa hypophysealis
N	Nasion, anterior point at the frontonasal suture
ANS	Anterior nasal spine, most anterior point of the nasal spine
PNS	Posterior nasal spine, most posterior point of the nasal spine
A	Deepest anterior point in the concavity of the anterior maxilla
B	Deepest anterior point in the concavity of the anterior mandible
Cd	Medial condylar point of the mandible
Cd′	A point that Pg projects onto the perpendicular line to the Cd–A line at the Cd point
Go	Gonion, a mid-plane point at the gonial angle located by bisecting the posterior and inferior borders of the mandible
Me	Menton, most inferior point of the chin bone
Ba	Basion, most posteroinferior point on the clivus
G	Most posterior point on the symphysis of the mandible
Pg	Prognathion, most anterior point on the symphysis of the mandible
P	Lowest point of the soft palate
TT	Most anterior point of the tip of the tongue
H	Most anterosuperior point of the hyoid bone
V	Most antero-inferior point of the epiglottic fold
Pt	Intersection of the posterior pharyngeal wall and most inferior margin of the foramen rotundum
Gn	Gnathion, the most antero-inferior point of body chin
NL	Nasal line, a line through ANS and PNS
MP	Mandibular plane, a plane constructed from Me through Go
VL	A line across C3 and C4

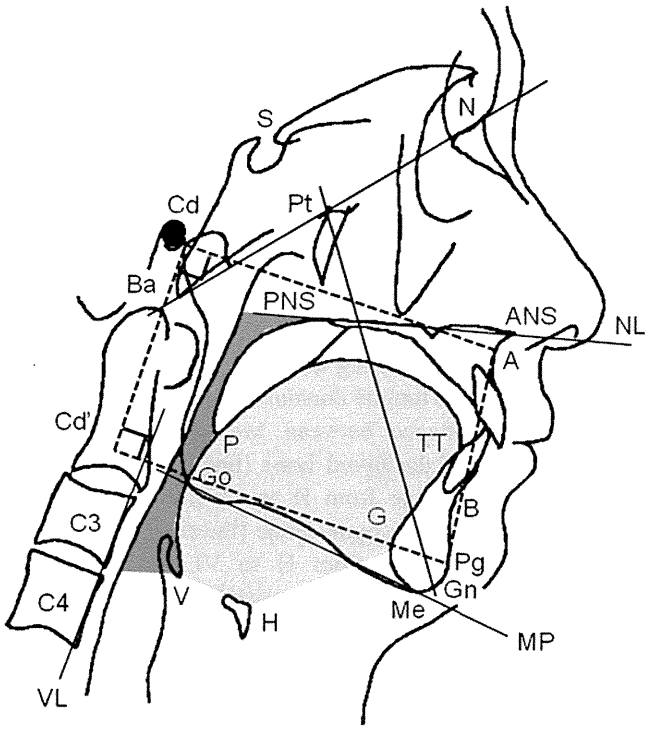

Fig. 1 Cephalometric landmarks and reference lines. For definitions, see Table 1. *Shaded area* indicates cross-sectional area of the tongue. *Dark-stained area* indicates cross-sectional area of the airway. *Lower face cage* was defined as a trapezoid formed by Cd–A–Pg–Cd′ (*dotted lines*)

the maxillomandibular enclosure size of the upper airway (cross-sectional area of the trapezoid enclosed by Cd–A–Pg–Cd′). Upper airway anatomical balance was assessed by the ratio between the tongue area and lower face cage as described in a previous study [5].

Pulmonary function tests

Pulmonary function tests were performed in the sitting position using CHESTAC (Chest M.I. Inc., Tokyo, Japan). Subjects underwent spirometric testing according to the recommended method [22]. Residual volume (RV) and total lung capacity (TLC) were measured by the closed circuit helium method, and diffusing capacity for carbon monoxide (DL_{CO}) was measured using a single-breath technique.

IOS

The assessment of respiratory impedance was performed by IOS (Masterscreen IOS-J, Jaeger, Wurzburg, Germany). IOS is different from the classical forced oscillation technique (FOT) because an impulse rather than a pseudo-random noise signal is applied by the loudspeaker. Data processing is also different between IOS and FOT. But IOS yields respiratory system resistance and reactance values similar to those provided by FOT [23]. Subjects were measured first in the sitting position and then in the supine position, fulfilling standard recommendations [24], as previously reported in detail elsewhere [25, 26]. In short, rectangular mechanical impulses containing the whole frequency spectrum were applied to the respiratory system through a mouthpiece while the patient was breathing quietly. The resulting pressure and flow signals were analyzed for amplitude, and the impedance (Z) represents the total mechanical load of the subject's respiratory system from which the resistance (R) and the reactance (X) of the respiratory system can be derived. The frequency range of the signal was from 5 to 35 Hz. The impedance at 5 Hz (Z5) represents the impedance of the total respiratory system. In the present study, we used respiratory resistance at 5 and 20 Hz (R5 and R20) as indices of total and proximal airway resistance, respectively. In IOS, low frequency oscillations are transmitted to the lung periphery, while those at frequencies ≥20 Hz are thought to be damped out before reaching the peripheral airways [27]. The reactance at 5 Hz (X5) may be determined by homogeneous distribution of ventilation, effective ventilation capacity, and compliance of the lung and chest wall. These indices have been shown to be useful for the evaluation of upper airway patency in OSA [12, 13].

Statistics

All statistical analyses were performed using StatView version 5.0 for Windows (Abacus Concepts, Berkeley, CA, USA). Continuous variables are expressed as means ± standard deviation (SD). Intra-observer agreement for the cephalometric measurements was evaluated by the intra-class correlation coefficient (ICC) [28]. The natural logarithm of the AHI was used as the dependent variable since the absolute values were not distributed normally. Chi-square tests were used to compare dichotomous variables and unpaired Student's t tests were used to compare continuous data between two groups. Relationships between two variables were analyzed by Pearson's correlation coefficient tests. Stepwise multiple regression analyses were performed to identify variables that could best explain AHI. A p value less than 0.05 was considered to indicate statistical significance.

Results

Relative contributions of obesity, craniofacial structure, pulmonary function, and IOS measurements to AHI in all subjects

Patient characteristics and polysomnographic data are shown in Table 2. The study group of 134 patients comprised 19

Table 2 Clinical characteristics and polysomnographic data on 134 patients

Age (years)	56.5±14.5
BMI (kg/m^2)	26.5±4.2
Neck circumference (cm)	40.2±3.2
Smoking history (current/ex/never)	37/70/27
Brinkman index	528±603
AHI (events/h)	26.0±22.5
Logarithmic AHI	2.8±1.3
Minimum SpO_2 (%)	79.0±10.5
SpO_2 <90% time/TST (%)	14.8±21.4
$PaCO_2$ (kPa)	5.6±0.5
PaO_2 (kPa)	11.4±1.5
A-aDO_2 (kPa)	1.6±1.5

Data presented as mean ± SD

BMI body mass index, *AHI* apnea/hypopnea index, *TST* total sleep time, *$PaCO_2$* arterial partial pressure of carbon dioxide, *PaO_2* arterial partial pressure of oxygen, *A-aDO_2* alveolar–arterial oxygen tension difference

Table 3 Stepwise multiple regression analysis to predict AHI (n=134)

	r^2
Age (years)	0.08
BMI (kg/m^2)	0.09
Neck circumference (cm)	–
PaO_2 (kPa)	–
A-aDO_2 (kPa)	–
Tongue area (cm^2)	–
PNS–P (mm)	–
TGL (mm)	–
MP-H (mm)	0.05
ERV (L)	–
%ERV (% pred)	–
R5 (kPa/L/s)	–
Z5[a] (kPa/L/s)	–
R5[a] (kPa/L/s)	–
R20[a] (kPa/L/s)	0.06
Cumulative r^2	0.28

AHI apnea/hypopnea index, *BMI* body mass index, *PaO_2* arterial partial pressure of oxygen, *A-aDO_2* alveolar–arterial oxygen tension difference, *ERV* expiratory reserve volume

[a] In the supine position

non-OSA, 32 mild OSA, 37 moderate OSA, and 46 severe OSA patients. Regarding cephalometric measurements, intra-observer agreement was excellent (ICC ranged from 0.92 to 0.99) for all variables except for ANB and TGL, which had good intra-observer agreement (ICC=0.82 in ANB and 0.83 in TGL). We investigated the associations between anthropometric variables, arterial blood gas data, cephalometric parameters, pulmonary function, IOS measurements, and AHI. The AHI had a significant positive correlation with age (r=0.26, p=0.003), BMI (r=0.32, p=0.0002), neck circumference (r=0.33, p=0.0001), and A-aDO_2 (r=0.37, p< 0.0001) and a negative correlation with PaO_2 (r=−0.31, p= 0.0003) (Table E1). Examination of cephalometric parameters showed that the AHI had a significant positive correlation with the tongue area (r=0.18, p=0.04), PNS–P (r=0.30, p=0.0004), TGL (r=0.23, p=0.008), and MP–H (r=0.28, p=0.001) (Table E2). Regarding pulmonary function, there was a significant negative correlation between the AHI and only with the expiratory reserve volume (ERV) (r=−0.28, p=0.001) and %ERV (r=−0.24, p=0.007) (Table E3). The results of IOS measurements revealed that the AHI had a significant positive correlation with R5 (r=0.22, p=0.01) in the sitting position and Z5 (r= 0.19, p=0.03), R5 (r=0.24, p=0.006), and R20 (r=0.25, p= 0.004) in the supine position (Table E3).

Stepwise multiple regression analysis was performed to examine the relationships with AHI using the preselected variables that were significantly related to AHI in the above analyses (Table 3). Age, BMI, MP–H by cephalometry, and R20 in the supine position on IOS significantly explained 28% of the variance in AHI [r^2 (coefficient of determination)=0.08, 0.09, 0.05, and 0.06, respectively].

Relative contributions of obesity, craniofacial structure, pulmonary function, and IOS measurements to the AHI based on the severity of OSA

We then compared the predominant determinants of AHI between 83 moderate-to-severe (AHI≥15) and 51 non-to-mild (AHI<15) OSA subjects. The clinical characteristics and polysomnographic data for these patients are shown in Table 4. The BMI and neck circumference were significantly higher, and the PaO_2 was significantly lower in moderate-to-severe OSA than in non-to-mild OSA (p= 0.007, 0.002, and 0.004, respectively). As we did for the overall group of 134 patients, we performed stepwise multiple regression analyses to account for AHI in the moderate-to-severe and the non-to-mild groups, using the preselected variables that were significantly related to AHI. They included BMI, neck circumference, PaO_2, A-aDO_2, R5 and R20 in the sitting position, and Z5, R5, and R20 in the supine position in moderate-to-severe OSA and included age, $PaCO_2$, VC, ERV, FEV_1, RV/TLC, and $\%DL_{CO}$ in non-to-mild OSA. In moderate-to-severe OSA, neck circumference and R20 in the supine position on IOS (r^2=0.11 and 0.10, respectively) significantly explained 21% of the variance in AHI. By contrast, in non-to-mild OSA, age and ERV (r^2=0.19 and 0.10, respectively) significantly explained 29% of the variance in AHI.

Table 4 Comparison of clinical characteristics and polysomnographic data between groups based on the severity of OSA

	AHI≥15 (n=83)	AHI<15 (n=51)	p value
Age (years)	57.6±12.3	54.7±17.4	0.26
BMI (kg/m^2)	27.2±4.6	25.2±3.2	0.007
Neck circumference (cm)	40.9±3.5	39.1±2.3	0.002
Smoking history (current/ex/never)	18/46/19	9/24/18	0.18
Brinkman index	578±595	446±613	0.22
AHI (events/h)	38.1±20.6	6.5±4.4	<0.0001
Logarithmic AHI	3.5±0.5	1.5±1.2	<0.0001
Minimum SpO_2 (%)	74.5±10.4	86.3±5.0	<0.0001
SpO_2 <90% time/TST (%)	22.9±23.7	1.6±2.4	<0.0001
$PaCO_2$ (kPa)	5.6±0.5	5.7±0.4	0.32
PaO_2 (kPa)	11.1±1.4	11.9±1.5	0.004
A-aDO_2 (kPa)	1.9±1.4	1.0±1.5	0.0008

Data presented as mean ± SD. Unpaired t tests were performed except for the chi-square test for smoking history

BMI body mass index, *AHI* apnea/hypopnea index, *TST* total sleep time, *$PaCO_2$* arterial partial pressure of carbon dioxide, *PaO_2* arterial partial pressure of oxygen, *A-aDO_2* alveolar–arterial oxygen tension difference

Relative contributions of obesity, craniofacial structure, pulmonary function, and IOS measurements to AHI based on the magnitude of obesity

We then compared the predominant determinants of AHI between 79 obese (BMI≥25) and 55 nonobese (BMI<25) subjects. The clinical characteristics and the polysomnographic data on these patients are shown in Table 5. There was a trend for more current smokers or ex-smokers to be present among the obese subjects. Neck circumference and the mean AHI were significantly higher, and the PaO_2 was significantly lower in obese subjects than in nonobese subjects (p<0.0001, p=0.002, and p<0.0001, respectively). We also performed stepwise multiple regression analyses to account for AHI in obese and nonobese subjects using the preselected variables that were significantly related to AHI. They included BMI, neck circumference, PaO_2, A-aDO_2, PNS–P, TGL, MP-H, ERV, and R5 and R20 in the sitting and supine positions in obese subjects and age and A-aDO_2 in nonobese subjects. In obese subjects, A-aDO_2, MP-H by cephalometry, and R20 in the sitting position on IOS (r^2=0.08, 0.10, and 0.07, respectively) significantly accounted for 25% of the variance in AHI. In contrast, in nonobese subjects, age alone was significantly related to AHI (r^2=0.25).

Discussion

We simultaneously analyzed the interrelationships between OSA and obesity, anatomical abnormalities measured by cephalometry, and functional abnormalities measured by pulmonary function testing and IOS. By multiple regression analysis, we found that age, BMI, MP-H by cephalometry, and R20 on IOS significantly contributed to AHI. In addition, separate analyses revealed that significant determinants of OSA differed between moderate-to-severe OSA and non-to-mild OSA and between obese subjects and nonobese subjects.

In addition to age and obesity (BMI), an anatomical abnormality (inferior displacement of the hyoid bone) and a functional abnormality (increased proximal airway resis-

Table 5 Comparison of clinical characteristics and polysomnographic data between groups based on the magnitude of obesity

	BMI≥25 (n=79)	BMI<25 (n=55)	p value
Age (years)	55.9±13.2	57.3±16.3	0.58
BMI (kg/m^2)	28.9±3.7	22.9±1.4	<0.0001
Neck circumference (cm)	41.7±3.0	38.1±2.2	<0.0001
Smoking history (current/ex/never)	19/44/16	8/26/21	0.02
Brinkman index	611±618	408±566	0.054
AHI (events/h)	31.0±25.6	18.9±14.6	0.002
Logarithmic AHI	3.0±1.2	2.5±1.3	0.03
Minimum SpO_2 (%)	77.1±11.5	81.8±8.2	0.009
SaO_2 <90% time/TST (%)	20.7±25.5	6.3±8.2	<0.0001
$PaCO_2$ (kPa)	5.6±0.5	5.6±0.4	0.47
PaO_2 (kPa)	10.9±1.5	12.0±1.4	<0.0001
A-aDO_2 (kPa)	2.1±1.4	0.9±1.4	<0.0001

Data presented as mean ± SD. Unpaired t tests were performed except for the chi-square test for smoking history

BMI body mass index, *AHI* apnea/hypopnea index, *TST* total sleep time, *$PaCO_2$* arterial partial pressure of carbon dioxide, *PaO_2* arterial partial pressure of oxygen, *A-aDO_2* alveolar–arterial oxygen tension difference

tance) were significantly related to OSA. Obesity and age have been considered to be the characteristic risk factors for OSA [29]. On the other hand, certain forms of craniofacial abnormalities measured by cephalometry [3–5], reduced lung volume [8–11], and increased upper airway resistance [12, 13] also have been suggested as predisposing factors for upper airway obstruction during sleep. Although these factors may be significantly affected by age and obesity [15–17, 30, 31], the relative contributions of anatomical and functional abnormalities, age, and obesity to OSA have remained to be elucidated. Our findings indicate that OSA is the result of independent interrelationships among anatomical abnormalities, functional abnormalities, age, and obesity, which reflects a multi-factorial pathophysiological feature of OSA.

We found that, compared with pulmonary function, airway resistance on IOS was related more closely to AHI. Structurally, the pharyngeal airway is surrounded by soft tissue, which is enclosed by bony structures and is caudally pulled by the thorax. As has been suggested, an imbalance between the amount of soft tissue and the size of the surrounding bony structures [32] and decreased thoracic traction [33] due to a reduced lung volume may result in increased tissue pressure surrounding the pharyngeal airway and decreased longitudinal tension of the pharyngeal airway wall, leading to increased upper airway resistance. Moreover, airway resistance was shown to increase when the body position changed from a sitting to a supine position [34]. In nonobese subjects, the falls in lung volume in a supine position are likely to lead to increased airway resistance, while in obese subjects in a supine position, such falls are smaller than in nonobese subjects and can only partly explain an increase in airway resistance [34]. Hence, there must be additional causes and sites of increased airway resistance in obese subjects. Our results showed the importance and usefulness of demonstrations of increased airway resistance on IOS in explaining the severity of OSA.

In one subgroup analysis, predominant determinants of AHI differed depending on the severity of OSA. In moderate-to-severe OSA, neck circumference and airway resistance were predominantly related to AHI, whereas in non-to-mild OSA, age and ERV were predominantly related to AHI. There was no overlap in those factors that were significantly associated with AHI, indicating a different pathogenesis of the disease between moderate-to-severe versus non-to-mild OSA. Asians were reported to have more severe OSA than Caucasians even when the BMI was similar between the two groups [7]. Our results indicate the importance of increased fat deposition adjacent to the upper airway rather than total body fat volume in Japanese individuals with moderate-to-severe OSA, which may partially explain this difference. Although it has been suggested that the consequences of craniofacial abnormalities are more severe in Japanese than in Caucasian OSA patients [3], craniofacial abnormalities were not significantly related to AHI in both moderate-to-severe and non-to-mild OSA groups in the present study after adjustment for other risk factors, although further study is needed. Moreover, that age independently correlated with non-to-mild OSA but not moderate-to-severe OSA may partly support the evidence that with increasing age, OSA prevalence increases but that its severity does not [19, 29].

Another subgroup analysis showed that in obese subjects, A-aDO_2, the distance between the hyoid bone and mandible, and airway resistance were predominantly related to AHI. Recent studies suggested that subclinical lung injury may be present in OSA possibly through local oxidative stress in the alveolus [35, 36]. Although the magnitude of the injury might not be great, given the effect of ventilation–perfusion inequality due to obesity [16], A-aDO_2 can be significantly related to AHI in obese OSA subjects. The position of the hyoid bone is correlated with accumulations of adipose tissue in pharyngeal regions, and its inferior displacement may give rise to the posterior relocation of the tongue and reduce upper airway patency [3, 37, 38]. Abdominal fat is likely to have direct effects on the downward movement of the diaphragm and is associated with increased airway resistance through the reduction in lung volume [16, 39]. Our results may also imply the importance of abundant parapharyngeal and intraabdominal distribution of adipose tissue in obese subjects. Additionally, in nonobese subjects, age alone had a significant relationship with the AHI. The unexplained variance by age may be related to structural or functional abnormalities that were not measured, indicating the complicated pathogenesis of OSA in lean individuals.

Unfortunately, the four crucial features in our study account for only 28% of the variance in AHI. There are several possible explanations. Firstly, various determinants of OSA, not limited to obesity, might be characteristic in Japanese subjects. Secondly, all of our anatomical and functional measurements were obtained during wakefulness, which may have limited relevance to the sleeping state. Furthermore, some cephalometric measurements, including that of the position of the hyoid bone, may be affected by muscle contraction required for central occlusion of the jaw. Thirdly, we did not evaluate the degree of ventilatory control stability. It is termed "loop gain", whose increase is suggested to play an important role in the pathogenesis of OSA [40, 41]. Additional assessments might have explained a certain proportion of the residual variance in AHI.

As a limitation, the present study had a small sample size (especially non-OSA subjects) with only male subjects from one university hospital, which might have limited the

generalization of the results. Moreover, we only studied Japanese subjects and did not directly assess inter-ethnic differences in OSA risk factors. Considering that OSA is highly prevalent worldwide, inter-ethnic differences in OSA risk factors is an important issue. Although we discussed inter-ethnic differences by comparing the results with previous studies, such as those of a recent study by Lee et al. [7], further studies directly comparing OSA risk factors in different ethnic groups would more clearly elucidate those risk factors. Another limitation is that we assessed craniofacial structures only by cephalometry. Our limited measures of craniofacial morphology may underestimate the actual contributions of craniofacial morphology, especially of upper airway anatomical imbalance. Additional three-dimensional, volumetric evaluations using computed tomography [42] or magnetic resonance imaging [43] might show more sensitively the impact of anatomical imbalance on the pathogenesis of OSA.

OSA is a multi-factorial disease in which age and obesity play important roles. However, aside from age and obesity, our results indicated that both anatomical and functional abnormalities play significant roles in the pathogenesis of OSA. The severity of OSA or obesity appears to determine the relative contribution of these abnormalities to sleep-related collapse of the upper airway.

Role of funding sources Kazuo Chin has received grants from the Japanese Ministry of Education, Culture, Sports, Science and Technology (nos. 20590921 and 22590760), Respiratory Failure Research Group and Health Science Research Grants (Comprehensive Research on Life-Style Related Diseases including Cardiovascular Diseases and Diabetes Mellitus) from the Ministry of Health, Labor and Welfare of Japan, and the Japan Vascular Disease Research Foundation.

References

1. Hudgel DW (1992) Mechanisms of obstructive sleep apnea. Chest 101:541–549
2. Ryan CM, Bradley TD (2005) Pathogenesis of obstructive sleep apnea. J Appl Physiol 99:2440–2450
3. Sakakibara H, Tong M, Matsushita K, Hirata M, Konishi Y, Suetsugu S (1999) Cephalometric abnormalities in non-obese and obese patients with obstructive sleep apnoea. Eur Respir J 13:403–410
4. Yu X, Fujimoto K, Urushibata K, Matsuzawa Y, Kubo K (2003) Cephalometric analysis in obese and nonobese patients with obstructive sleep apnea syndrome. Chest 124:212–218
5. Tsuiki S, Isono S, Ishikawa T, Yamashiro Y, Tatsumi K, Nishino T (2008) Anatomical balance of the upper airway and obstructive sleep apnea. Anesthesiology 108:1009–1015
6. Dempsey JA, Skatrud JB, Jacques AJ, Ewanowski SJ, Woodson BT, Hanson PR, Goodman B (2002) Anatomic determinants of sleep-disordered breathing across the spectrum of clinical and nonclinical male subjects. Chest 122:840–851
7. Lee RW, Vasudavan S, Hui DS, Prvan T, Petocz P, Darendeliler MA, Cistulli PA (2010) Differences in craniofacial structures and obesity in Caucasian and Chinese patients with obstructive sleep apnea. Sleep 33:1075–1080
8. Heinzer RC, Stanchina ML, Malhotra A, Fogel RB, Patel SR, Jordan AS, Schory K, White DP (2005) Lung volume and continuous positive airway pressure requirements in obstructive sleep apnea. Am J Respir Crit Care Med 172:114–117
9. Tagaito Y, Isono S, Remmers JE, Tanaka A, Nishino T (2007) Lung volume and collapsibility of the passive pharynx in patients with sleep-disordered breathing. J Appl Physiol 103:1379–1385
10. Bradley TD, Martinez D, Rutherford R, Lue F, Grossman RF, Moldofsky H, Zamel N, Phillipson EA (1985) Physiological determinants of nocturnal arterial oxygenation in patients with obstructive sleep apnea. J Appl Physiol 59:1364–1368
11. Appelberg J, Nordahl G, Janson C (2000) Lung volume and its correlation to nocturnal apnoea and desaturation. Respir Med 94:233–239
12. Lin CC, Wu KM, Chou CS, Liaw SF (2004) Oral airway resistance during wakefulness in eucapnic and hypercapnic sleep apnea syndrome. Respir Physiol Neurobiol 139:215–224
13. Cao J, Que C, Wang G, He B (2009) Effect of posture on airway resistance in obstructive sleep apnea–hypopnea syndrome by means of impulse oscillation. Respiration 77:38–43
14. Dempsey JA, Veasey SC, Morgan BJ, O'Donnell CP (2010) Pathophysiology of sleep apnea. Physiol Rev 90:47–112
15. Mayer P, Pepin JL, Bettega G, Veale D, Ferretti G, Deschaux C, Levy P (1996) Relationship between body mass index, age and upper airway measurements in snorers and sleep apnoea patients. Eur Respir J 9:1801–1809
16. Salome CM, King GG, Berend N (2010) Physiology of obesity and effects on lung function. J Appl Physiol 108:206–211
17. Zerah F, Harf A, Perlemuter L, Lorino H, Lorino AM, Atlan G (1993) Effects of obesity on respiratory resistance. Chest 103:1470–1476
18. Watson RA, Pride NB (2005) Postural changes in lung volumes and respiratory resistance in subjects with obesity. J Appl Physiol 98:512–517
19. Ohdaira F, Nakamura K, Nakayama H, Satoh M, Ohdaira T, Nakamata M, Kohno M, Iwashima A, Onda A, Kobayashi Y, Fujimori K, Kiguchi T, Izumi S, Kobayashi T, Shinoda H, Takahashi S, Gejyo F, Yamamoto M (2007) Demographic characteristics of 3,659 Japanese patients with obstructive sleep apnea–hypopnea syndrome diagnosed by full polysomnography: associations with apnea–hypopnea index. Sleep Breath 11:93–101
20. Rechtschaffen A, Kales A (1968) A manual of standardized terminology, techniques and scoring system for sleep stages of human subjects. National Institutes of Health, Washington
21. Iber C, Ancoli-Israel S, Chesson A, Quan S (2007) The AASM manual for the scoring of sleep and associated events: rules, terminology and technical specifications. American Academy of Sleep Medicine, Westchester
22. Miller MR, Hankinson J, Brusasco V, Burgos F, Casaburi R, Coates A, Crapo R, Enright P, van der Grinten CP, Gustafsson P, Jensen R, Johnson DC, MacIntyre N, McKay R, Navajas D, Pedersen OF, Pellegrino R, Viegi G, Wanger J (2005) Standardisation of spirometry. Eur Respir J 26:319–338
23. Hellinckx J, Cauberghs M, De Boeck K, Demedts M (2001) Evaluation of impulse oscillation system: comparison with forced oscillation technique and body plethysmography. Eur Respir J 18:564–570
24. Oostveen E, MacLeod D, Lorino H, Farre R, Hantos Z, Desager K, Marchal F (2003) The forced oscillation technique in clinical practice: methodology, recommendations and future developments. Eur Respir J 22:1026–1041
25. Takeda T, Oga T, Niimi A, Matsumoto H, Ito I, Yamaguchi M, Matsuoka H, Jinnai M, Otsuka K, Oguma T, Nakaji H, Chin K, Mishima M (2010) Relationship between small airway function

and health status, dyspnea and disease control in asthma. Respiration 80:120–126
26. Haruna A, Oga T, Muro S, Ohara T, Sato S, Marumo S, Kinose D, Terada K, Nishioka M, Ogawa E, Hoshino Y, Hirai T, Chin K, Mishima M (2010) Relationship between peripheral airway function and patient-reported outcomes in COPD: a cross-sectional study. BMC Pulm Med 10:10
27. Goldman MD, Saadeh C, Ross D (2005) Clinical applications of forced oscillation to assess peripheral airway function. Respir Physiol Neurobiol 148:179–194
28. Bédard M, Martin NJ, Krueger P, Brazil K (2000) Assessing reproducibility of data obtained with instruments based on continuous measurements. Exp Aging Res 26:353–365
29. Young T, Shahar E, Nieto FJ, Redline S, Newman AB, Gottlieb DJ, Walsleben JA, Finn L, Enright P, Samet JM (2002) Predictors of sleep-disordered breathing in community-dwelling adults: the Sleep Heart Health Study. Arch Intern Med 162:893–900
30. Pecora NG, Baccetti T, McNamara JA Jr (2008) The aging craniofacial complex: a longitudinal cephalometric study from late adolescence to late adulthood. Am J Orthod Dentofacial Orthop 134:496–505
31. Janssens JP (2005) Aging of the respiratory system: impact on pulmonary function tests and adaptation to exertion. Clin Chest Med 26:469–484
32. Watanabe T, Isono S, Tanaka A, Tanzawa H, Nishino T (2002) Contribution of body habitus and craniofacial characteristics to segmental closing pressures of the passive pharynx in patients with sleep-disordered breathing. Am J Respir Crit Care Med 165:260–265
33. Van de Graaff WB (1988) Thoracic influence on upper airway patency. J Appl Physiol 65:2124–2131
34. Michels A, Decoster K, Derde L, Vleurinck C, Van de Woestijne KP (1991) Influence of posture on lung volumes and impedance of respiratory system in healthy smokers and nonsmokers. J Appl Physiol 71:294–299
35. Lederer DJ, Jelic S, Basner RC, Ishizaka A, Bhattacharya J (2009) Circulating KL-6, a biomarker of lung injury, in obstructive sleep apnoea. Eur Respir J 33:793–796
36. Aihara K, Oga T, Harada Y, Chihara Y, Handa T, Tanizawa K, Watanabe K, Tsuboi T, Hitomi T, Mishima M, Chin K (2011) Comparison of biomarkers of subclinical lung injury in obstructive sleep apnea. Respir Med 105(6):939–945
37. Guilleminault C, Riley R, Powell N (1984) Obstructive sleep apnea and cephalometric roentgenograms. Am Rev Respir Dis 130:145–146
38. Maltais F, Carrier G, Cormier Y, Series F (1991) Cephalometric measurements in snorers, non-snorers, and patients with sleep apnoea. Thorax 46:419–423
39. Begle RL, Badr S, Skatrud JB, Dempsey JA (1990) Effect of lung inflation on pulmonary resistance during NREM sleep. Am Rev Respir Dis 141:854–860
40. White DP (2005) Pathogenesis of obstructive and central sleep apnea. Am J Respir Crit Care Med 172:1363–1370
41. Verbraecken JA, De Backer WA (2009) Upper airway mechanics. Respiration 78:121–133
42. Shigeta Y, Ogawa T, Ando E, Clark GT, Enciso R (2011) Influence of tongue/mandible volume ratio on oropharyngeal airway in Japanese male patients with obstructive sleep apnea. Oral Surg Oral Med Oral Pathol Oral Radiol Endod 111:239–243
43. Saigusa H, Suzuki M, Higurashi N, Kodera K (2009) Three-dimensional morphological analyses of positional dependence in patients with obstructive sleep apnea syndrome. Anesthesiology 110:885–890

ELSEVIER

The Journal of
Heart and Lung
Transplantation
http://www.jhltonline.org

INNOVATION

Living-donor lobar lung transplantation with sparing of bilateral native upper lobes: A novel strategy

Takuji Fujinaga, MD,[a] Toru Bando, MD,[a] Daisuke Nakajima, MD,[a] Jin Sakamoto, MD,[a] Fengshi Chen, MD,[a] Tsuyoshi Shoji, MD,[a] Hiroaki Sakai, MD,[a] Hisanari Ishii, MD,[b] Senri Miwa, MD,[c] and Hiroshi Date, MD[a]

From the Departments of [a]Thoracic Surgery, [b]Anesthesiology and [c]Cardiovascular Surgery, Kyoto University Graduate School of Medicine, Kyoto, Japan.

KEYWORDS:
living-donor;
lung transplantation;
size mismatch;
native lung sparing;
three-dimensional CT
volumetric evaluation

A 44-year-old man became wheelchair-bound due to sever bronchiolitis obliterans caused by peripheral blood stem cell transplantation for acute myelogenous leukemia. His lung donors, his sister and his wife, were 17 cm shorter than him. He successfully underwent living-donor lobar lung transplantation with sparing of the bilateral native upper lobes to address the size mismatch. Ten months after the transplantation, the patient has returned to a normal lifestyle without supplemental oxygen.
J Heart Lung Transplant 2011;30:351–3

Living-donor lobar lung transplantation (LDLLT) has been established as an alternative procedure to cadaveric lung transplantation for patients who cannot wait for a brain-dead donor. In LDLLT, 1 lower lung lobe donated from each of 2 donors (total of 2 lobes) is implanted into the recipient after bilateral pneumonectomy. The size of the donor lobar lungs is the most critical issue influencing the result of LDLLT. According to a formula previously reported, an acceptable predictive donor lung size compared with a recipient's predictive forced vital capacity (FVC) is >45% to 50%.[1] In the case of a large patient, especially an adult male, there can be a large size disparity between the donor lung size and recipient's chest cavity because grafts may be too small. These size issues often prevent large adult male patients from undergoing LDLLT.

Herein we report the first case of a successful LDLLT in which a very large size mismatch between donor lungs and recipient chest cavity was solved by sparing the bilateral native upper lobes.

Reprint requests: Hiroshi Date, MD, Department of Thoracic Surgery, Kyoto University Graduate School of Medicine, 54 Shogoin Kawahara-cho, Sakyo-ku, Kyoto 606-8507, Japan. Telephone: +81-75-751-3835. Fax: +81-75-751-4647.
E-mail address: hdate@kuhp.kyoto-u.ac.jp

Case report

A 44-year-old man was diagnosed with acute myelogenous leukemia (AML) in May 2007. He received chemotherapy followed 6 months later by a peripheral blood stem cell transplantation (PBSCT) from his human leukocyte antigen (HLA)-serotype-matched sister. In November 2008, he experienced dyspnea with exertion and shortness of breath. A chest computed tomography (CT) and pulmonary function test indicated the development of bronchiolitis obliterans due to chronic graft-vs-host disease of PBSCT. His respiratory distress progressed despite medications such as steroids, immunosuppressive agents and inhaled bronchodilators and he became wheelchair-bound with supplemental oxygen. He was referred to Kyoto University Hospital for possible LDLLT in September 2009, as the average waiting time for cadaveric lung transplantation is about 3 years in Japan. His acute myeloid leukemia (AML) had remained in complete remission for 21 months.

The candidates for lung donation in this case included his sister, who was the blood stem cell donor for the PBSCT, and his wife. The ratio of calculated graft FVC to predicted FVC of the recipient was 45.7%. Although the ratio was adapted to our criteria, there was a 17-cm difference in height between the patient and both donors (the patient's height was 170 cm and both donors were 153 cm). Three-

1053-2498/$ -see front matter
doi:10.1016/j.healun.2010.10.006

dimensional CT volumetric evaluation showed the recipient chest cavity to be 6,189 ml (right 3,318 ml, left 2,871 ml) and the donor grafts' volume to be 1,745 ml (right 715 ml, left 1,030 ml). Therefore, the ratio of the donor grafts' volume to recipient's chest cavity was only 28%. Pre-operative chest CT (Figure 1A) and pulmonary ventilation perfusion scintigraphy revealed homogeneous impairment in all the lobes of the recipient and no infectious lesions were found in the recipient's lungs.

The surgical options were discussed repeatedly with the patient and his family, and they were willing to proceed with LDLLT, with sparing of the bilateral native upper lobes, which they understood to be an experimental procedure. The case was carefully discussed and approved by the ethics committee of our hospital.

Through a clamshell incision, lingual segmentectomy and bilateral hilar dissection were performed to avoid bleeding by heparinization during cardiopulmonary bypass (CPB). After establishing CPB, a right middle lower lobectomy and left lower lobectomy were performed. The patient's older sister and wife were the right and left lung donors, respectively. The donor lobar lungs were immediately flushed with cooled ET–Kyoto solution (Otsuka Pharmaceuticals, Japan) after harvest. The right graft was implanted followed by left graft implantation. The bronchus was anastomosed using a continuous suture technique with a 4-0 PDS suture (Ethicon, Somerville, NJ). The pulmonary vein and artery were sutured with 6-0 Prolene (Ethicon). The spared bilateral upper lobes were ventilated to avoid atelectasis throughout the operation except during bronchial anastomosis. Both grafts were reventilated and reperfused essentially at the same time. Weaning from CPB was completed within 15 minutes after reperfusion and without difficulty.

The patient's post-operative course was uneventful. The recipient was weaned from mechanical ventilation on post-operative day (POD) 3, and he left the intensive care unit on POD 12. Withdrawal of oxygen inhalation was completed on POD 28. Excellent bronchial healing was obtained bilaterally. At 6-month evaluation, dramatic improvements were observed for pulmonary function, arterial blood gas, 6-minute walk distance and symptoms (Table 1). Of note, forced expiratory volume in 1 second (FEV_1) increased from 590 to 2,090 ml. Post-operative chest CT revealed well-expanded donor lungs and spared native lungs with no detectable dead space in the bilateral chest cavities (Figure 1B). Post-operative pulmonary ventilation scintigraphy demonstrated that marked air trapping remained in the spared lungs (Figure 2A). Post-operative perfusion scintigraphy showed little perfusion to the spared lungs (Figure 2B).

Table 1 Patient Data

	Pre-transplant	Post-transplant (6 months)
Body size		
Height (cm)	171	171
Weight (kg)	52	54.0
Spirometry		
FVC (ml)	2,790	3,700
FVC (%)	72.3	95.3
FEV_1 (ml)	590	2,090
$FEV_{1\%}$ (%)	21.1	56.5
DLCO (ml/min/mm Hg)	10	18.4
DLCO (%)	35.0	64.1
Arterial blood gas	Room air	Room air
PaO_2 (mm Hg)	60.1	86.9
$PaCO_2$ (mm Hg)	57.0	36.4
6-minute walk	NA	603
MMRC dyspnea scale	4	1

DLCO, diffusion capacity for carbon monoxide; FEV_1, forced vital capacity in 1 second; FVC, forced vital capacity; MMRC, Modified Medical Research Council; NA, not analyzed.

Discussion

Size matching is the most critical issue in LDLLT because it involves only 2 lower lobes, which the recipient receives from 2 donors.[1,2] Therefore, it is often difficult for large patients to find 2 donors who can donate enough lung volume. Most of the recipients who have undergone LDLLT in Japan were children or women.[2] In fact, we have

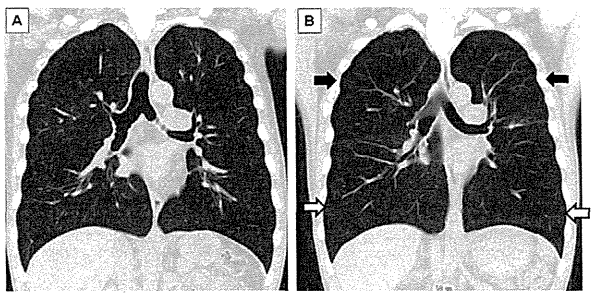

Figure 1 Coronal view of CT. (A) Pre-operative CT showed homogeneous hyperlucent lung consisting with typical findings of bronchiolitis obliterans. (B) Post-operative CT shows spared native lungs (black arrows) and implanted donor lungs (white arrows).

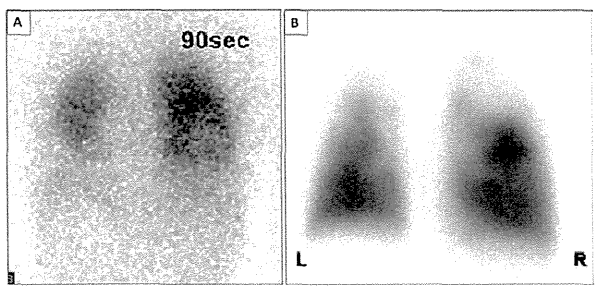

Figure 2 Postero-anterior view of post-operative differential ventilation/perfusion lung scan. (A) ^{133}X washout imaging at 90 seconds demonstrates marked air trapping in the native spared upper lobes. (B) Tc99m macroaggregated albumin perfusion lung scan demonstrates that the spared native lungs received little perfusion and the implanted small grafts received a majority of the pulmonary blood flow.